water

MDPI

Article

Apparent Friction Coefficient Used for Flow Calculation in Straight Compound Channels

Elżbieta Kubrak, Janusz Kubrak *, Adam Koziol, Adam Kiczko and Marcin Krukowski

Faculty of Civil- and Environmental Engineering, Warsaw University of Life Sciences-SGGW, 02-787 Warsaw, Poland; elzbieta_kubrak@sggw.pl (E.K.); adam_koziol@sggw.pl (A.K.); adam_kiczko@sggw.pl (A.K.); marcin_krukowski@sggw.pl (M.K.)

* Correspondence: janusz_kubrak@sggw.pl; Tel.: +48-22-593-5275

Received: 28 March 2019; Accepted: 7 April 2019; Published: 10 April 2019

Abstract: Water flow in channels with a compound cross-section involves an exchange of water mass and momentum between the slower flowing water in the floodplains and the faster water in the main channel. This process is called the streams interaction. As a result, the water velocity in the main channel decreases, and at the same time the velocity and depth of flow increase in the part of the floodplains adjacent to the main channel. Diversification of the surface roughness of the main channel and floodplains significantly affects the form of interactions. The results of laboratory experiments were used to characterize the influence of interactions on the discharge capacity of the channel with diversified roughness. The reduction in velocity of the main channel caused by the stream interactions is described with the apparent friction coefficients introduced at the boundary between the main channel and the floodplain. The obtained values of resistance coefficients, supplemented with the values from experiments reported in the literature, were used to establish a relationship useful in assessing the discharge capacity of such channels.

Keywords: compound channels; interaction of stream; apparent friction coefficient

1. Introduction

For the practice, the kinematic structure of the stream in the channel with a compound cross-section can be characterized with sufficient accuracy, as the distribution of the depth averaged velocity in the cross-section. This distribution depends on the channel shape in the plane, the shape of the cross-section, the roughness of the side slopes and the bottom of the main channel, and flow resistance caused by the turbulent exchange of water masses and momentum between slower flowing water in the floodplains, and faster in the main channel. The process of the momentum exchange, along with the formation of eddy structures in the transition region between floodplains and the main channel was called the "kinematic effect" [1], and nowadays is described as the streams interaction. As a result of the interaction, the water velocity in the main channel decreases, while the velocity and depth of flow increase in parts of the floodplains adjacent to the main channel [2]. Diversification of the surface roughness of the main channel and the floodplains intensifies the process of creating eddies and secondary flows in the main channel, and affects the capacity of the channel with a compound cross-section [3–6]. Despite the spatial nature of the phenomena, in practice, many different methods are used to assess the discharge capacity of channels with compound cross-sections, and many calculation programs for the water profile in the channels are based on one-dimensional models [7]. Among them, the Divided Channel Method (DCM) is most often mentioned. The phenomenon of interaction emerging in the transition region between the main channel and the floodplain is described by separating the two streams, most often with vertical lines, on which the apparent shear stresses were

assigned. The concept of the apparent tangential stresses at the division boundaries of the channel compound cross-sections was introduced by Wright and Carstens (1970) [8].

From the eighties of the last century, a number of formulas have been introduced to calculate the flow resistance due to the momentum transfer between the main channel and floodplain, according to concept of the apparent shear stress [9–13]. They were elaborated as a result of hydraulic experiments on the channel, using small and large scale models. A review of formulas derived to describe apparent tangential stresses at the boundary of streams in the main channel and floodplains can be found in Moreta and Martin-Vide (2010) [14].

The knowledge of apparent shear stresses makes it possible to determine the values of the dimensionless resistance coefficients used to calculate the average velocity in the steady uniform flow in the main channel of the compound cross-section, using the Darcy-Weisbach formula:

$$v_m = \sqrt{\frac{8gR_mS_o}{f_m}} \tag{1}$$

where: v_m—average flow velocity in the main channel, g—gravitational acceleration, f_m—resistance coefficient for the main channel cross-section, calculated for the wetted perimeter, accounting for the length of the cross-section division plane, side slopes and the bottom of the main channel, R_m—hydraulic radius of the main channel cross-section, S_o—longitudinal channel slope.

The flow resistance coefficients at the division boundary of the compound cross-section, according to Nuding (1998) [15], calculated on the basis of apparent shear stresses, depend on the following parameters of the channel (Figure 1):

$$f_a = f\left(f_{mb};\ \frac{H}{h_f};\ \frac{b_m}{b_f};\ 1:m;\ \frac{k_{mb}}{k_{fb}}\right) \tag{2}$$

where: f_a—apparent coefficient of resistance at the boundary between the main channel and floodplain area, f_{mb}—resistance coefficient of the main channel bottom, f_{ms}—resistance coefficient of the main channel side slopes, f_m—resistance coefficient in the main channel, f_{fb}—resistance factor of the bottom of the floodplain, H—water depth in the main channel, h_f—water depth in the floodplain, b_m—bottom width of the main channel, b_f—floodplain width, 1:m—aspect of the side slope of the main channel and floodplains, k_{mb}—absolute surface roughness of the main channel, k_{ms}—absolute roughness of the main channel side slopes, k_{fb}—absolute surface roughness of the floodplain, k_{fs}—absolute roughness of the floodplain side slopes.

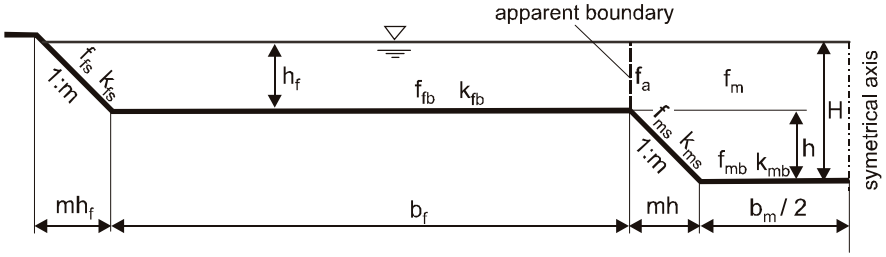

Figure 1. Symbols used for dimensions of the compound cross-section of the channel.

Bretschneider and Özbek T (1997) [16] used measurements of average water velocity in the main channel, and apparent tangential stresses at the division boundary of the cross-section on large-scale hydraulic models, as part of the SERC (Science and Engineering Research Council) program at the Hydraulic Research Laboratory in Wallingford, England, to determine the apparent resistance coefficients on vertical division lines, discussed in this work. The goal of the present study and performed hydraulic experiments was to explain how the surface roughness of the main channel and floodplains affects the values of these coefficients.

2. Study on Discharge Capacity of Channel with Compound Cross-Section

Study on the capacity of the channel with the compound cross-section was carried out in the hydraulic laboratory of the Department of Water Engineering of the Warsaw University of Life Sciences on a concrete model of a rectilinear section of the channel with a constant slope of 0.5‰.

The channel with a compound trapezoidal cross-section was 16 m long and 2.10 m wide (Figure 2). The bottom of the main channel and symmetrical floodplains in the cross-section were horizontal. The channel model was supplied by five pumps with a total discharge of 0.50 m^3/s in a closed water cycle. In the initial section of the channel, a row of 0.30 m long PVC (Polyvinyl Chloride) pipes was laid, calming the flow, and directing water into the model. At the end of the channel, a tilting gate for controlling the water levels was mounted, which was used to force a steady uniform flow into the channel. Measured values were the water depths in the main channel and in the floodplains, the flow velocity at the cross-section points, the water temperature, and the flow rate in the channel. Measurements of the water flow velocity were carried out in a section located halfway along the channel. To measure the velocity components, an 11 × 33 mm ellipsoid electrostatic PEMS was installed on a sliding measuring carriage. Spot velocity measurements were carried out with an accuracy of 1 cm/s in 77 measuring profiles (Figure 2), and in nearly 500 cross-section points. The required length of the measurement time series for the longitudinal velocity was determined in the respect of an error of the calculated mean longitudinal velocity, with an allowable absolute error of the mean velocity of δ = 1 cm/s. It was found that the velocity should be measured 50 times, in order to give a 5 s measurement period with 0.1 s interval, using the electromagnetic probe. The water depths were measured with a pin gauge having an accuracy of 0.1 mm. To measure the flow rate in the channel, a calibrated circular measuring overflow with a diameter of 540 mm was used. The water head on the length of the channel was measured with a differential pressure gauge, based on the difference in water levels in piezometers located in the bottom axis of the main channel, at a distance of 4.0 m and 12.0 m from the beginning of the channel. The electro-probe and differential pressure gauge were connected to a computer measurement logger.

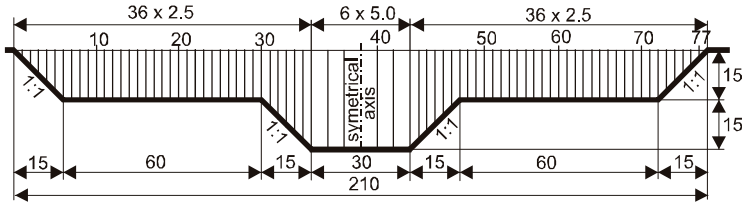

Figure 2. Location of measurement points in the cross-section (dimensions in cm).

Diversification of the surface roughness in the channel was obtained by painting the concrete of a blurred surface with paint (called a smooth surface), or by applying a terrazzo layer with a grain diameter of 6–12 mm (called a rough surface).

Channel capacity experiments were carried out for the following variants (Figure 3):

- variant 1.0 (W 1.0): Smooth surface of the main channel and floodplains
- ($k_{mb} = k_{ms} = k_{fb} = k_{fs}$ = 0.00005 m),
- variant 2.0 (W 2.0): Smooth surface of the main channel and rough surface of floodplains ($k_{mb} = k_{ms}$ = 0.00005 m, $k_{fb} = k_{fs}$ = 0.0089 m)
- variant 3.0 (W 3.0): Smooth surface of the bottom of the main channel and rough surface of the sides slopes of the main channel and floodplains (k_{mb} = 0.00005 m, $k_{ms} = k_{fb} = k_{fs}$ = 0.0089 m).

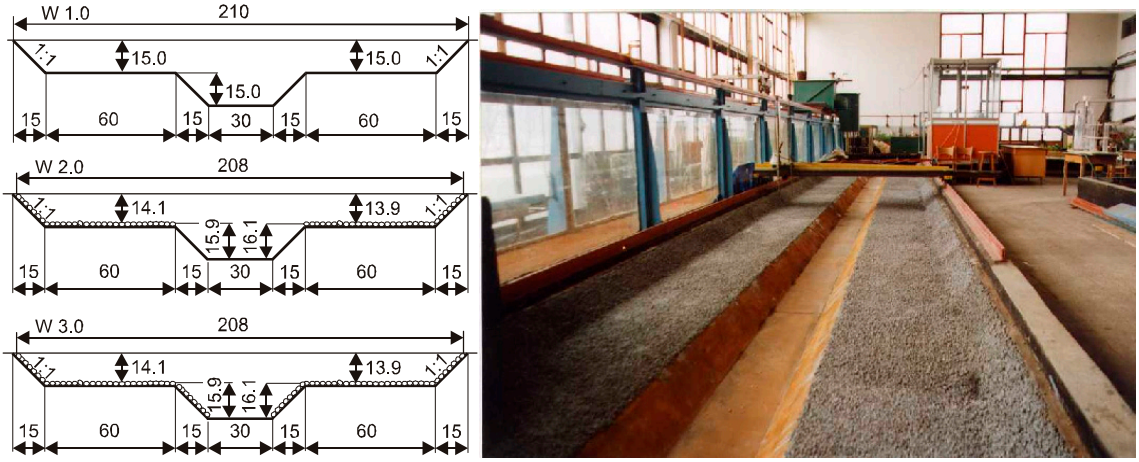

Figure 3. Cross-section schema of the channel in the analyzed variants (dimensions in cm) and a view of the channel model in the variant W 2.0.

Values of the absolute roughness of flume surfaces were determined from the distribution of mean velocity in the region where it satisfies the log-law [17].

The list of experiments carried out during the experiments, measured flow rates in the main channel and the adjacent floodplains, is summarized in Table 1.

Table 1. Experimental variants with stream interactions.

Case	Water Depth H (m)	Discharge (m^3/s)			Reynolds Numbers Re	
		Q	in the Main Channel Q_m	in the Left Floodplain Q_{fl}	in the Main Channel Re_m	in the Left Floodplain Re_{fl}
Variant W 1.0						
1.0.1	0.1690	0.0340	0.0309	0.0020	156,969	12,354
1.0.2	0.1720	0.0359	0.0318	0.0028	160,279	16,873
1.0.3	0.1725	0.0359	0.0319	0.0029	160,574	17,467
1.0.4	0.1727	0.0385	0.0320	0.0029	160,994	17,765
1.0.5	0.1808	0.0449	0.0346	0.0051	170,486	30,686
1.0.6	0.1825	0.0454	0.0352	0.0056	172,695	33,269
1.0.7	0.1845	0.0482	0.0359	0.0061	175,241	36,407
1.0.8	0.1860	0.0502	0.0364	0.0066	177,012	38,965
1.0.9	0.1965	0.0613	0.0405	0.0098	191,890	56,708
1.0.10	0.2063	0.0734	0.0447	0.0131	206,829	74,354
1.0.11	0.2151	0.0876	0.0488	0.0162	221,149	90,642
1.0.12	0.2330	0.1038	0.0581	0.0233	252,707	125,497
1.0.13	0.2445	0.1212	0.0649	0.0283	275,174	149,105
1.0.14	0.2532	0.1317	0.0703	0.0323	292,497	167,410
Variant W 2.0						
2.0.1	0.1885	0.0369	0.0313	0.0016	152,611	9884
2.0.2	0.2026	0.0416	0.0321	0.0035	150,882	20,444
2.0.3	0.2096	0.0468	0.0338	0.0047	156,352	27,235
2.0.4	0.2227	0.0549	0.0371	0.0075	166,371	42,344
2.0.5	0.2330	0.0625	0.0401	0.0100	175,729	54,980
2.0.6	0.2395	0.0685	0.0430	0.0118	185,742	63,946
2.0.7	0.2508	0.0808	0.0481	0.0150	202,824	79,827
2.0.8	0.2630	0.0947	0.0531	0.0172	218,135	89,331
Variant W 3.0						
3.0.1	0.1858	0.0291	0.0246	0.0014	125,934	8248
3.0.2	0.2022	0.0359	0.0271	0.0038	133,052	22,438
3.0.3	0.2135	0.0429	0.0292	0.0056	139,513	32,121
3.0.4	0.2258	0.0505	0.0325	0.0084	150,784	47,286
3.0.5	0.2366	0.0599	0.0384	0.0116	173,558	63,629
3.0.6	0.2506	0.0704	0.0412	0.0145	180,196	77,303
3.0.7	0.2622	0.0805	0.0447	0.0178	190,355	92,574
3.0.8	0.2758	0.0932	0.0507	0.0229	210,226	116,197

On the basis of spot velocity measurements it was possible to plot lines of constant velocities (isovels) in the cross-sections of the channel. Examples of isovels for the experiment variant W 1.0, W 2.0 and W 3.0 at similar water depths are shown in Figure 4.

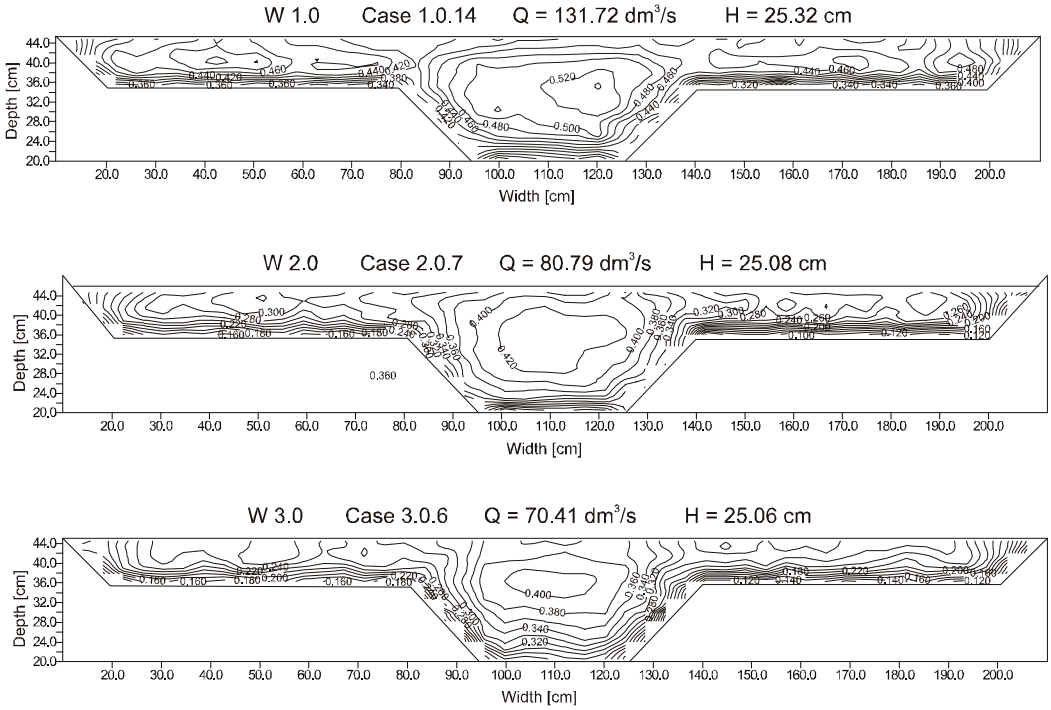

Figure 4. Isovels in the cross-section of the channel for selected experiments in different experimental variants at similar depth.

3. Resistance Coefficients in the Main Channel

The values of dimensionless resistance coefficients in the main channel with different bottom and slope roughness, as well as resistance factors f_a in the plane of distribution of the cross-section of the channel, were calculated using the Einstein method (1934) [18]. According to this method, for each surface roughness along the perimeter of the cross-section the flow area can be found, in which this roughness shapes the flow conditions. The area can be determined using the graph of isovels in the cross-section of the main channel. The division of the cross-section into these areas is carried out with lines perpendicular to the isovels, starting from the wetted perimeter points, separating the perimeter into sections with different roughness (Figure 5). This technique for determining division lines assumes that they are free from the shear stress, and forces are not transferred between the separated areas.

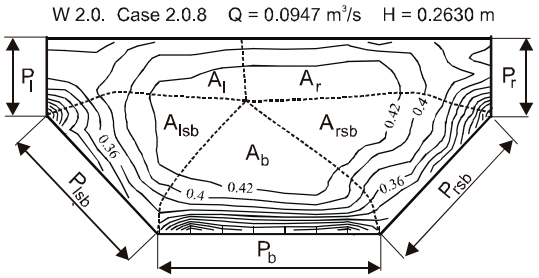

Figure 5. Surface areas of stream cross-sections A_i in which the flow conditions are shaped under the influence of a constant roughness over the length of the wetted perimeter P_i.

According to Einstein, the average flow velocity in each of these sections is equal to the average velocity across the entire main channel cross-section, i.e., $v_i = v_m$. Expressing the velocity with the Darcy-Weisbach equation with this condition, the following dependence can be obtained:

$$\sqrt{\frac{8gR_iJ}{f_i}} = \sqrt{\frac{8gR_mJ}{f_m}} \tag{3}$$

then:

$$f_i = f_m \frac{R_i}{R_m} \tag{4}$$

where: f_m denotes the average Darcy's friction factor in a main channel—being the substitutionary coefficient of resistance for the cross-section of the main channel calculated for the wetted perimeter P_m that includes lengths of the section dividing lines ($P_m = P_l + P_{lsb} + P_b + P_{rsb} + P_r$), R_m symbolizes the hydraulic radius of the entire cross-section of the main channel (R_m=A_m/P_m), and R_i is the hydraulic radius of the cross-sectional area per given roughness ($R = A_i/P_i$).

The coefficient of resistance f_m in the cross-section of the main channel is calculated on the basis of the average velocity ($v_m = Q_m/A_m$) and the calculated hydraulic radius of the main channel R_m.

The determined areas of the cross-sectional area A_i, in which the flow conditions are shaped under the influence of a constant roughness over the length of the wetted P_i perimeter, were used to calculate the hydraulic radius R_i and the coefficients of resistance f_i.

The values of apparent resistance coefficients calculated in this way, as well as the resistance coefficients of the bottom and left slope of the main channel, are summarized in Table 2.

Table 2. Cross-section areas A_i for sections of the wetted perimeter with a constant roughness, hydraulic radius R_i and flow resistance coefficients in the cross-section of the main channel determined on the basis of the isovels.

Case	A_l (m^2)	R_l (m)	f_a (-)	A_{lsb} (m^2)	R_{lsb} (m)	f_{ms} (-)	A_b (m^2)	R_b (m)	f_{mb} (-)
Variant W 1.0									
1.0.1	0.015	0.772	0.1982	0.014	0.064	0.0164	0.0237	0.079	0.0203
1.0.2	0.016	0.734	0.1854	0.014	0.064	0.0163	0.0236	0.079	0.0199
1.0.3	0.016	0.725	0.1833	0.013	0.059	0.0150	0.0238	0.080	0.0201
1.0.4	0.016	0.726	0.1835	0.012	0.058	0.0145	0.0244	0.081	0.0206
1.0.5	0.017	0.558	0.1346	0.013	0.062	0.0150	0.0258	0.086	0.0207
1.0.6	0.018	0.546	0.1306	0.013	0.063	0.0152	0.0251	0.084	0.0200
1.0.7	0.018	0.528	0.1251	0.012	0.058	0.0138	0.0265	0.088	0.0209
1.0.8	0.019	0.527	0.1237	0.012	0.059	0.0138	0.0261	0.087	0.0204
1.0.9	0.020	0.429	0.0936	0.014	0.066	0.0143	0.0302	0.101	0.0220
1.0.10	0.023	0.401	0.0809	0.016	0.075	0.0151	0.0275	0.092	0.0185
1.0.11	0.022	0.331	0.0619	0.019	0.087	0.0164	0.0305	0.102	0.0190
1.0.12	0.026	0.311	0.0496	0.019	0.088	0.0140	0.0354	0.118	0.0188
1.0.13	0.028	0.300	0.0431	0.020	0.096	0.0138	0.0326	0.109	0.0157
1.0.14	0.031	0.296	0.0394	0.018	0.086	0.0115	0.0373	0.124	0.0165
Variant W 2.0									
2.0.1	0.017	0.636	0.2083	0.012	0.053	0.0174	0.031	0.105	0.0342
2.0.2	0.017	0.402	0.1501	0.015	0.065	0.0244	0.036	0.120	0.0447
2.0.3	0.019	0.384	0.1403	0.015	0.065	0.0239	0.037	0.122	0.0446
2.0.4	0.019	0.300	0.1054	0.018	0.079	0.0276	0.038	0.127	0.0447
2.0.5	0.021	0.297	0.0994	0.019	0.083	0.0278	0.039	0.130	0.0436
2.0.6	0.024	0.302	0.0940	0.018	0.078	0.0243	0.037	0.125	0.0388
2.0.7	0.025	0.283	0.0784	0.019	0.085	0.0234	0.039	0.130	0.0361
2.0.8	0.034	0.331	0.0835	0.019	0.082	0.0207	0.039	0.128	0.0324
Variant W 3.0									
3.0.1	0.015	0.614	0.2945	0.013	0.056	0.0269	0.029	0.097	0.0467
3.0.2	0.015	0.372	0.1823	0.017	0.073	0.0356	0.031	0.102	0.0501
3.0.3	0.015	0.291	0.1403	0.018	0.080	0.0388	0.033	0.110	0.0530
3.0.4	0.017	0.270	0.1208	0.019	0.082	0.0368	0.037	0.123	0.0550
3.0.5	0.023	0.308	0.1109	0.019	0.081	0.0293	0.036	0.119	0.0430
3.0.6	0.024	0.266	0.0959	0.023	0.099	0.0358	0.034	0.114	0.0411
3.0.7	0.024	0.234	0.0800	0.023	0.101	0.0346	0.038	0.127	0.0433
3.0.8	0.028	0.247	0.0735	0.023	0.101	0.0300	0.039	0.131	0.0389

The calculated values of apparent resistance coefficients f_a and resistance coefficients of the main channel f_m as well as of the bottom f_{mb}, the left side slope of the main channel, f_{ms}, the bottom of the left floodplain f_{fb}, of the compound cross section in experiments made in variants W 1.0, W 2.0 and W 3.0, are presented as a function of the depth ratio H/h_f in Figure 6.

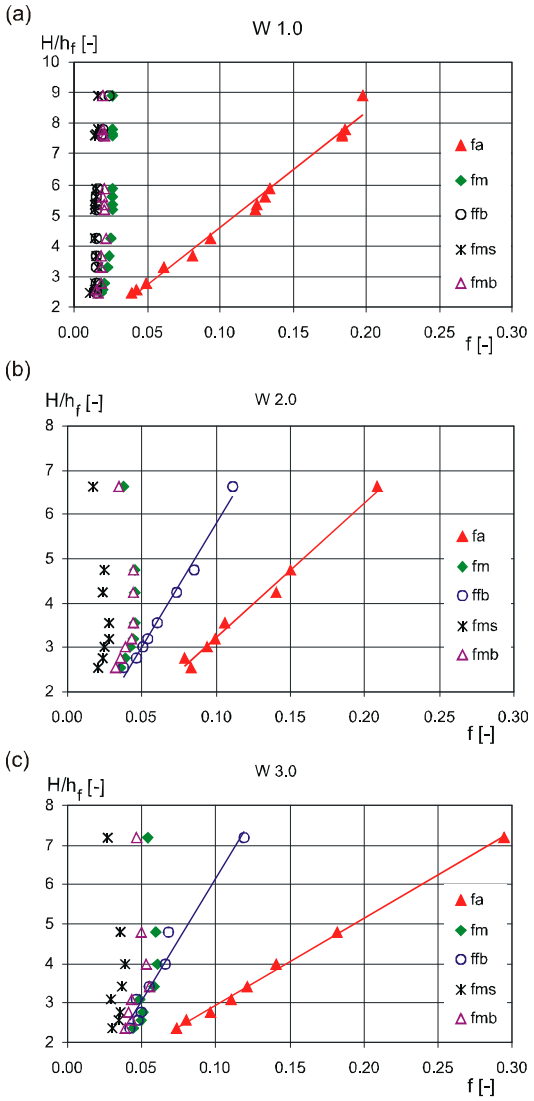

Figure 6. Variability of resistance coefficients in the cross-section of the compound cross-section in variants W 1.0 (**a**), W 2.0 (**b**) and W 3.0 (**c**). Note: for (**a**), $f_a = 0.0262\frac{H}{h_f} - 0.0199$, $R^2 = 0.989$, $f_{fb} = 0.0169$, $f_{ms} = 0.0147$, $f_{mb} = 0.0195$, $f_m = 0.0246$. for (**b**), $f_a = 0.0324\frac{H}{h_f} - 0.0043$, $R^2 = 0.989$, $f_m = 0.0169$; $f_{fb} = 0.0718\frac{H}{h_f} - 0.0030$, $R^2 = 0.988$, $f_{ms} = 0.0211$, $f_{mb} = 0.0355$. for (**c**), $f_a = 0.0430\frac{H}{h_f} - 0.0280$, $R^2 = 0.998$, $f_m = 0.0535$; $f_{fb} = 0.0153\frac{H}{h_f} - 0.004$, $R^2 = 0.963$, $f_{ms} = 0.0535$, $f_{mb} = 0.0464$.

The values of the apparent resistance coefficients for the compound cross-section in variants W 1.0, W 2.0 and W 3.0, and resistance coefficients of the bottom of the flood plain f_{fb} with high roughness (in variants W 2.0 and W 3.0) decrease with the increase of the flow depth (with reduction of the ratio H/h_f). Changes in these resistance coefficients are explained with linear regression equations and are shown in Figure 6. In contrast, values of resistance coefficients for the entire main channel f_m, f_{ms} slopes and bottom of the main channel f_{mb} in all variants of the study and the floodplain f_{fb} in the W 1.0 variant, do not change significantly with depth, which is why their average values were calculated (Figure 6).

The effect of the surface roughness of the floodplains, slopes and bottom of the main channel and the depth of the water flow on the values of the apparent resistance coefficients f_a in the analyzed experiment variants are shown in Figure 7.

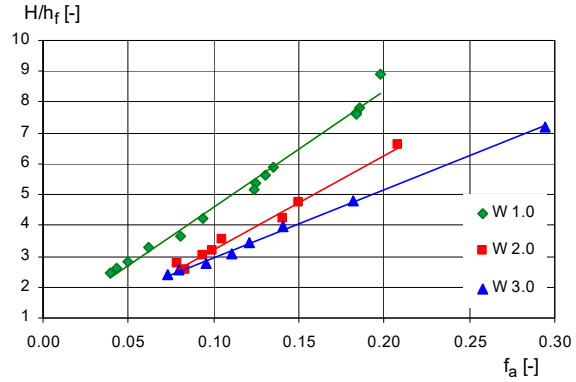

Figure 7. Variability of apparent resistance coefficients in a compound channel cross-section in variants W 1.0, W 2.0 and W 3.0 as a function of the flow depth.

Figure 7 shows that the increase in floodplain roughness in the variant W 2.0 in relation to the variant W 1.0 resulted in an almost two-fold increase in the apparent resistance coefficients at the same flow depths in the channel. The additional increase in roughness of the main channel side slopes in the W 3.0 variant did not significantly affect the increase of these coefficients compared to the W 2.0 variant, but only at large flow depths $2 < H/h_f < 3$. A clear effect appeared at low flow depths, and so with $H/h_f \approx 7$, the apparent coefficient of resistance in the variant W 3.0 was 0.290, and was almost 0.07 more than in the variant W 2.0, which was 0.220. Such a rapid increase in the value of apparent resistance coefficients in the variant W 2.0 in relation to the W 1.0 can be explained by the magnitude of changes in the depth average velocity in the main channel and in the floodplain (Figure 8). If the values of the apparent resistance coefficients are all the greater, the greater are the differences between the flow velocities in the main channel and the floodplain.

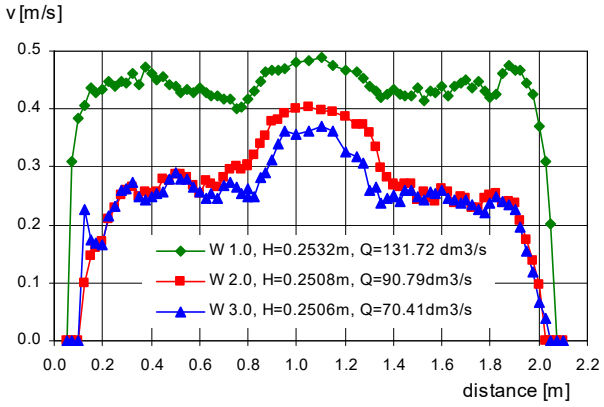

Figure 8. Distribution of average velocity in verticals in W 1.0, W 2.0 and W 3.0 variants with similar flow depths in the channel.

The variability of the apparent resistance coefficients is expressed in relation to the resistance coefficients of the bottom of the main channel f_a/f_{mb}. Pasche (1984) [19], and later German DVWK guidelines (1991) [20] recommended in the calculations of the capacity of channels with compound cross-sections using DCM for the ratio of depths in the main channel and floodplains fulfilling the condition $H/h_f > 3$, the value of the apparent resistance coefficient equal to $f_a = 3f_{mb}$. However, at depths meeting the condition $H/h < 3$, it is recommended to take the value of the apparent resistance coefficient on the cross-section lines equal to the resistance coefficient of the bottom $f_a = f_{mb}$.

Figure 9 presents the variability of ratios of the apparent resistance coefficients to the coefficients of the bottom of the main channel f_a/f_{mb} in respect of the relative depth H/h_f obtained from the conducted experiments.

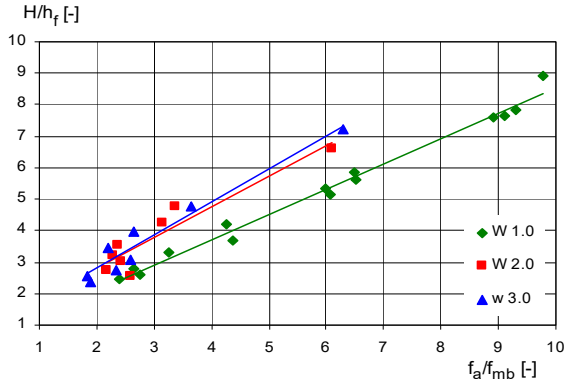

Figure 9. Values of resistance coefficients in the division plane and bottom of the main channel f_a/f_{mb} as function of relative depth H/h_f.

As shown in Figure 9, with the ratio of the depth in the main channel and the floodplain $3 < H/h_f < 7$ in the variant W 1.0, the apparent resistance coefficients took values $f_a = (3 \div 8) f_{mb}$ The introduction of rough floodplain in the variant W 2.0, and the side slopes of the main channel in the variant W 3.0, caused that at $3 < H/h_f < 7$, the values of the apparent resistance coefficients become equal.

Since the values of the apparent resistance coefficients also depend on the width of the floodplain and the main channel (2), it was decided to identify such a dependence. This was done on the basis of results reported in the literature. Bretschneider and Özbek (1997) [16] calculated the apparent, and those for the bottom of the main channel, coefficients of resistance, on the basis of measured apparent shear stresses, in experiments performed on large scale models of a compound channel as part of the SERC program at the Hydraulic Research Laboratory in Wallingford, England. The ratios of apparent and bottom resistance coefficients from their own experiments in the variant W 1.0 were compared with the results of the Bretschneider and Özbek calculations (1997) [16] for a series of tests performed in a smooth two-section channel with 1:1 side slopes, and different ratios of floodplain and the main channel widths b_f/b_m, and these are shown in Figure 10. The dependencies presented there show that the increase in the width of the floodplain in relation to the width of the main channel significantly affects the discussed ratio of resistance coefficients. This effect decreases with the increase of the flow depth. The character of changes in the resistance coefficients of f_a/f_{mb} as a function of ratios of depth H/h_f and the widths of the floodplain and the main channel b_f/b_m from our own research, presented in Figure 10, is explained by the regression equation:

$$\frac{f_a}{f_{mb}} = \left(0.25\frac{b_f}{b_m} + 0.55\right)\frac{H}{h_f} \tag{5}$$

applicable for $0.8 \leq b_f/b_m < 4.6$ and $0 < H/h_f < 11$.

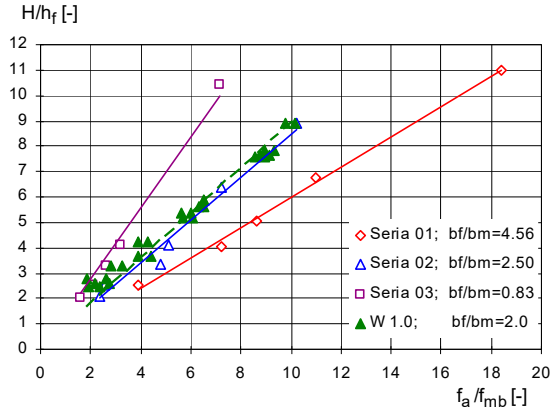

Figure 10. The values of the resistance coefficients of f_a/f_{mb} in the function of H/h_f from our own research in the variant W 1.0, together with the results of Bretschneider and Özbek (1997) [16] for a series of experiments performed in a two-section channel with side slopes of 1:1.

As it results from the Equation (5) for very narrow floodplains, with b_f/b_m = 1.0 and H/h_f = 3, the ratio of resistance coefficients takes the values f_a/f_{mb} = 2.4. However, for wide floodplains, with b_f/b_m = 4.5 and H/h_f = 3, the ratio of these coefficients reaches the value of f_a/f_{mb} = 5.0.

4. Conclusions

The analysis of the values of resistance coefficients determined for the main channel with the compound cross-section showed that:

- In a smooth channel with a compound cross-section, the values of the resistance coefficients of the bottom and side slopes of the main channel do not change significantly with an increase in depth; an increase in the surface roughness of the floodplain area causes the increase of resistance coefficients in the smooth main channel,
- the values of apparent resistance coefficients are several times greater than the resistance coefficients for side slopes and bottoms of the main channel and floodplains,
- apparent resistance coefficients decrease with increasing depth,
- the ratios of apparent, and the bottom of the main channel resistance coefficients, increase along with the increase in the width of the floodplain in relation to the width of the main channel.

Author Contributions: Conceptualization E.K. and J.K.; Methodology E.K. and J.K.; Software, E.K. and J.K.; Formal Analysis J.K. and E.K.; Investigation E.K., J.K., A.K. (Adam Kozioł) and M.K.; Writing-Original Draft Preparation, E.K., J.K. and A.K. (Adam Kiczko); Visualization, E.K.

Funding: This research was funded by the National Centre for Research and Development, grant number [347837/11/NCBR/2017], "Technological innovations and system of monitoring, forecasting and planning of irrigation and drainage for precise water management on the scale of drainage/irrigation system".

Conflicts of Interest: The authors declare no conflict of interest.

References

1. Zheleznakov, G.V. Interaction of channel and floodplain streams. In Proceedings of the 14th IAHR Congress, Paris 5, IAHR, Paris, France, 29 August–3 September 1971; pp. 145–148.
2. Kubrak, E.; Kubrak, J.; Kuśmierczuk, K.; Kozioł, A.; Kiczko, A.; Rowiński, P. Influence of stream interactions on the carrying capacity of two-stage channels. *J. Hydraul. Eng.* **2019**, *145*. [CrossRef]
3. Shiono, K.; Knight, D.W. Turbulent open-channel flows with variable depth across the channel. *J. Fluid Mech.* **1991**, *222*, 617–646. [CrossRef]
4. Tominaga, A.; Nezu, I. Turbulent structure in compound open-channel flows. *J. Hydraul. Eng.* **1991**, *117*, 21–41. [CrossRef]

5. Bousmar, D.; Zech, Y. Momentum transfer for practical flow computation in compound channels. *J. Hydraul. Eng.* **1999**, *125*, 696–706. [CrossRef]
6. Van Prooijen, B.C.; Booij, R.; Uijttewaal, W.S.J. Measurement and analysis methods of large scale coherent structures in a wide shallow channel. In Proceedings of the 10th International Symposium on Applications of Laser Techniques to Fluid Mechanics, Calouste Gulbenkian Foundation, Lisbon, Portugal, 10–13 July 2000.
7. Bousmar, D. Flow Modelling in Compound Channels. Momentum Transfer between Main Channel and Prismatic or Non-Prismatic Floodplains. Ph.D. Thesis, Université Catholique de Louvain, Louvain, Belgium, 2002.
8. Wright, P.R.; Carstens, H.R. Linear momentum flux to overbank section. *J. Hydraul. Div.* **1970**, *96*, 1781–1793.
9. Myers, W.R.C. Momentum Transfer in a Compound Channel. *J. Hydraul. Res.* **1978**, *2*, 139–150. [CrossRef]
10. Wormleaton, P.R.; Allen, J.; Hadjipanos, P. Discharge assessment in compound channel flow. *J. Hydraul. Div.* **1982**, *108*, 975–994.
11. Knight, D.W.; Demetriou, J.D. Flood plain and main channel flow interaction. *J. Hydraul. Eng.* **1983**, *109*, 1073–1092. [CrossRef]
12. Prinos, P.; Townsend, R.D. Comparison of methods for predicting discharge in compound open channels. *Adv. Water Res.* **1984**, *7*, 180–187. [CrossRef]
13. Christodoulou, G.C. Apparent shear stress in smooth compound channels. *Water Resour. Manag.* **1992**, *66*, 235–247. [CrossRef]
14. Moreta, P.J.M.; Martin-Vide, J.P. Apparent friction coefficient in straight compound channels. *J. Hydraul. Res.* **2010**, *48*, 169–177. [CrossRef]
15. Nuding, A. Zur Durchflußermittlung bei gegliederten Gerinnen. *Wasserwirtschaft* **1998**, *88*, 130–132.
16. Bretschneider, H.; Özbek, T. Durchflußermittlung bei geoemtrisch grgliedrten Gerinnen. *Wasserwirtschaft* **1997**, *87*, 4.
17. Nezu, I.; Nakagawa, H. *Turbulence in Open-Channel Flows*; IAHR Monograph, A. A. Balkema: Rotterdam, The Netherlands, 1993; p. 281.
18. Einstein, H.A. Der hydraulische Oder Profil-Radius. *Schweiz. Bauztg.* **1934**, *103*, 89–91.
19. Pasche, E. Turbulenzmechanismen in naturnahen Fließgewässern und die Möglichkeit ihrer mathematischen Erfassung. Ph.D. Thesis, RWTH Aachen, Aachen, Germany, 1984.
20. DVWK-Merkblätter. *220: Hydraulische Berechnung von Fließgewässern*; Verlag Paul Parey: Hamburg, Germany, 1991.